SELECTED PROJECTS ON DIRECT DETECTION OF WIMP DARK MATTER

ANGEL MORALES
Laboratory of Nuclear and High Energy Physics, University of Zaragoza, Pedro Cerbuna s/n 50009 Zaragoza, Spain
E-mail: amorales@posta.unizar.es

ABSTRACT

The strategies and techniques applied to the detection of WIMP dark matter are illustrated by several of their recent achievements. New projects are entering the stage to go a step further in the quest for WIMPs. A selection of them are presented and the next goals of various current experiments are reported.

1. Introduction

There exists substantial evidence that most of the universe does not shine and a compelling motivation to believe that its nature is mainly non-baryonic. Without entering into considerations about how much of this component is hot or cold to reproduce the power spectrum of density perturbations at all scales, and about how large the dark baryonic component of the galactic halo could be, it is taken for granted that there is enough room in our halo for cold dark matter in form of WIMPs (Weak Interacting Massive neutral Particles)[1)] or axions[2)] to justify a try for its detection[3,8)] either directly or through their by-products.

The attempts to directly detect WIMPs are based in the measure of the nuclear recoil which would be produced by the WIMP elastic scattering off the target nuclei[3,4,5)]. Many experimental efforts are underway with a variety of detectors and techniques[6,7,8)]. The current status of the field is reviewed by R. Bernabei in these Proceedings, whereas this overview will deal with the future plans of some running experiments and the perspectives of WIMP detection in a few selected projects to illustrate what is coming next.

Detectors used so far include semiconductor diodes (Ge, Si), scintillators (NaI, CaF_2, LqXe), cryogenic particle detectors (Ge, Si, Al_2O_3, TeO_2) but other novel experiments are entering the stage with new targets and techniques. Most of the results obtained till now have been extracted from the non-observance of WIMPs signal by simple comparison of the recorded background with the expected rate. Such comparison has served to exclude particle dark matter candidates or to constrain their properties for various masses, types of interactions and strengths, in terms of exclusion plots σ(m). Fig. 1a shows a typical set of exclusion plots obtained[7,8)] from various running experiments[9,10,11,12,13,14,15,16,17,38)]. The shaded area shows the expected values of σ(m) in various representative neutralino models[19,56)]. On the other hand, a seasonal modulation effect in the observed rate has been recently reported by the DAMA collaboration and attributed tentatively to a WIMP signal. Such

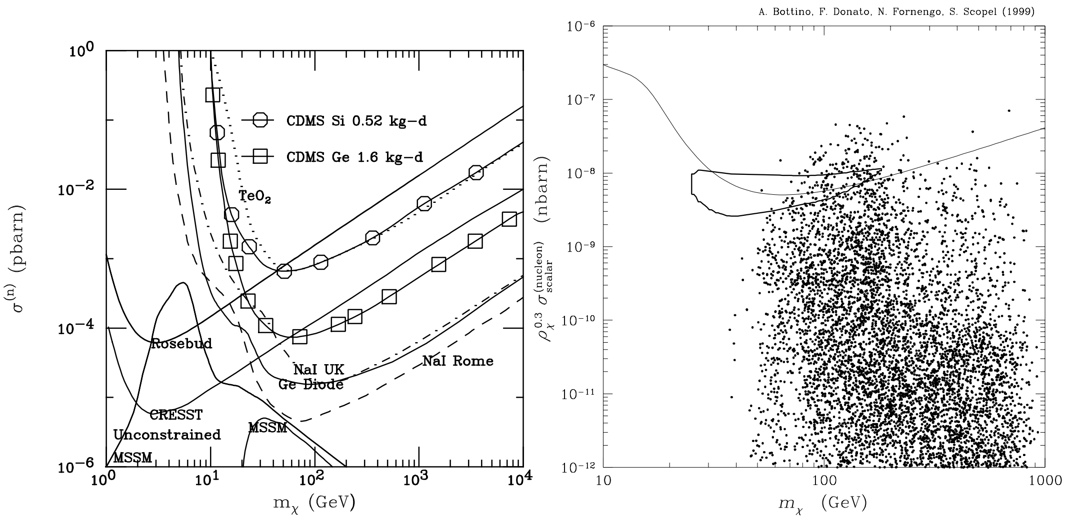

Figure 1: **(a)** Set of exclusion plots σ(m) obtained from various running experiments. **(b)** Region of cross-sections and masses of the DAMA candidate (2σ). The lines show the exclusion plots of Ge and NaI. The scatter dots indicate the neutralino MSSM predicions.

WIMP has been shown to be compatible with the particle physics and cosmology requirements for a neutralino[19]. Fig. 1b shows the region of the DAMA effect in the plot σ(m), together with a scatter plot of the neutralino expected cross-section[19].

We will first sketch the basic strategies followed and the main achievements accomplished up to now in WIMP searches to frame the main lines of approach which are pursued in future detectors.

2. Looking for WIMPs. General Strategies

WIMPS (m$\sim$GeV–TeV, $v \sim 10^{-3}$ c) hypothetically forming the galactic dark halos could make a nucleus recoil with a few keV (T$\sim$1–100 keV). Only a fraction of this energy is visible in the detector (depending on the type of detector and target and on the mechanism of energy deposition). The nuclear recoil ionization (or scintillation) efficiency relative to that of electrons make even more tiny the visible energy due to the WIMP interaction. A nuclear recoil of T keV in Germanium translates into 0.25T keV of electron equivalent energy (or a factor about 0.3 for Sodium, 0.09 for Iodine or 0.65 for Xenon in scintillators). Consequently, the imprints left by the WIMPs are expected to be of very small energy (keV range), requiring detectors of very small thresholds.

WIMPs interact with quarks within nucleons which are at their turn inside a nucleus. Consequently the WIMP-nucleus cross-section depends on the properties and parameters entering in such three levels of description. In the non-relativistic approximation, the WIMP-nucleus cross-section has two components: an spin-independent part (corresponding to the coupling of WIMP with the nuclear mass), and a spin-dependent part (due to the WIMP coupling to the nuclear spin). The Nuclear Physics for the spin-independent part is well described by a simple form factor. However, in the axial part detailed nuclear models are required.

The detection rate depends on magnitudes coming from the astrophysics, particle physics and nuclear physics domains: the dark matter halo model, the type of WIMP and interaction and the nuclear target, as well as on the detector itself. The wide choice of input parameters in the evaluation make the predicted rate encompass various orders of magnitude, a fact which does not facilitate the planning of an experiment.

The known weak strength of the WIMP interaction to provide the right relic density implies that WIMP detection rates are very small. Representative values of the expected rates[5,20)] per unit of detector mass and day stand roughly below $\mathrm{R} < 1 - 10^{-3}$ c/kg day for the more appealing type of WIMPs, the neutralino of the Minimal Supersymmetric extension of the Standard Model (MSSM)[21)]. The higher and smaller quoted bounds refer (respectively) to the spin-independent (scalar) and spin-dependent (axial) type of interactions. This small event rate lies moreover, as pointed out earlier, in the few keV region of the energy spectrum where the large background accumulated from the continua of all sources of radioactivity dominates.

The rarity and smallness of the WIMP signal dictate the experimental strategies for present and future detection.

1. Reduce the background down to the lowest possible value (controlling the radiopurity of the detector, its components and shielding). To avoid possible sources of contamination, some future detectors (HDMS[25)], GENIUS[26)], GEDEON[27)]) have planned to eliminate the materials close to the detectors (like cryostats or some components). The use of segmented detectors to perform efficient anticioincidence measurements is also a handy strategy (CUORE)[28)].

   To further reduce the remaining unavoidable intrinsic or cosmogenically-induced radioactivity, use discrimination mechanisms to distinguish electron recoils (tracers of the background) from nuclear recoils (originate by WIMPs or neutrons). This has been accomplished till now through statistical pulse shape analysis (PSD) in some experiments (DAMA[17)], UKDM[16)], SACLAY[22)]), or on an event-by-event basis in others (CDMS[23,6)], EDELWEISS[24)]), identifying in this case the nuclear recoils by measuring at the same time two different mechanisms of energy deposition, like the ionization and heat. The implementation of these particle identification mechanisms has been one of the main recent achievements in WIMP searches.

2. Make detectors of very low energy threshold and high efficiency to see most of the signal spectrum, not just the tail. Cryogenic particle detectors are good

devices for such purpose[29].

3. Select detectors with most favourable nuclear targets to optimize the WIMP energy deposition and rate (large nuclear factor-of-merit[30,5,31]) according to the type of interaction explored and to the damping effect produced in the rates by the form factors[31,32]. Large quenching factors are obviously a bonus.

The differential energy spectrum expected from the WIMP energy deposition is rather similar in shape to that of the ambient background. The level of background sets the lower limit of the constrain which one can put on the particle dark matter because those WIMPs which for given masses and interaction cross-sections lead to a theoretical spectrum above the observed background can be disregarded as dark matter components. Getting exclusion plots or constrains from the background spectrum is only a way of asserting what cannot be dark matter, but not what dark matter is. The radioactive background cannot be disentangled from a supposed WIMP signal unless WIMP identification signatures be provided. So it is imperative:

4. To look for distinctive signatures of the WIMP, not faked by the background or by instrumental artifact, to prove that you are seeing a WIMP. Identifying labels would be:

   - an annual modulation of the signal rate and energy spectrum (of a few percent) due to the seasonal June-December variation in the relative velocity Earth-halo[33].
   - a forward-backward asymmetry in the direction of the nuclear recoil due to the Earth motion through the halo[34].
   - the nuclear target dependence of the WIMP rate[4].

   The annual modulation signature has been already explored. Pioneering searches for WIMP annual modulation signals with NaI (Canfranc)[35] and LqXe (Gran Sasso)[36] resulted in constraints on masses and WIMPs couplings more stringent than that obtained from the total background spectrum. Also ELEGANTS in Kamioka searched for annual modulation signals[37].

   The DAMA experiment at Gran Sasso (using nine highly radiopure NaI scintillators of a total mass of about 100 kg), after an statistics of about 20000 kg day, has reported[18] an annual modulation effect at the 99.6% C.L. This effect has been interpreted as due to a WIMP of m = 59^{+17}_{-14} GeV and scalar cross-section on protons of $\sigma_p = \left(7.0^{+0.4}_{-1.2}\right) \times 10^{-6}$ picobarns (see Fig. 1b). It is obvious that current and future WIMP direct experiments plan to explore this m,σ region.

   As far as the other genuine signatures are concerned, various types of detectors sensitive to the nuclear recoil direction have been proposed but they are not yet operative. The signal dependence on the A number or spin of the target have not yet been exploited to identify the WIMP.

3. WIMP Searches. Where we stand, where we go

We will summarize now the main achievements accomplished in the techniques for WIMP detection and the prospects for their improvement.

3.1. Radiopurity selection

Ultralow background techniques and a thorough selection of the radiopurity of the materials have provided very low background levels in the raw background spectra obtained in the 5-50 keV region with various detectors.

Some results are B$\sim$ 0.1 $\sim$ 0.2 c/keV kg day at E$\sim$ 5 keV (PNL/USC/UZ)[38)] and B= 0.05 c/keV kg day at E$\sim$ 20 keV (H/M[12)], HDMS[25)]) with Germanium detectors. Results from high radiopurity NaI scintillators stand at the level of B$\sim$ 1 to 3 c/keV kg day (UKDMC[16)], DAMA[17)], SACLAY[22)]).

These limits might already be the closest to the ultimate limit in radiopurity selection in these detectors. The next step has been to identify the background and reject it.

3.2. Statistical Pulse Shape Discrimination (PSD)

The timing behaviour of the pulses can be used to statistically discriminate nuclear recoils from gamma background because of the shorter time constants of nuclear versus electron recoils. The data population which could be due to nuclear recoils (and so to neutrons and WIMPs) is reduced in this way one to two orders of magnitude (depending on the energy) from its measured level (1 to 3 c/keV kg day) to only a few 10^{-1} or 10^{-2} c/keV kg day, with different degree of success, depending on the experiment[16,17,22)].

By using these "PS discriminated" backgrounds, the σ(m) exclusion plots from NaI have surpassed that derived from the (raw) spectra obtained with the best Ge detectors. Some border regions of the MSSM neutralino parameter space have been consequently excluded (corresponding to scalar cross-section on protons above 10^{-5} pb for medium mass WIMPs) See Figures 1a and b.

3.3. Simulteanous measure of ionization and heat

Bolometers which also collect electron-hole pairs have allowed a very effective background discrimination by measuring simultaneously the heat and the ionization produced in the detector by the interacting particle. The energy released by the recoiling nucleus impinged by the WIMP (or the recoiling electron impinged by a particle) appears in form of phonons and electron-hole pairs. Simultaneous measurement of both quantities for each event allows the discrimination of electron recoil events from nuclear recoil events because for a given deposited energy—measured as phonons—the recoiling nucleus ionizes less than the electrons. This discrimination is quite effective between bulk gamma and nuclear recoil interactions. Typical results after phonon-ionization discrimination are B $\approx 0.1 \sim 0.3$ c/keV kg day recoil background (above 15–30 keV) out of a measured background of $2 \sim 4$ c/keV kg day in Germanium and Silicon bolometers (CDMS[6,23,40], EDELWEISS[24]). Recent results [6]using also phonon rise time to distinguish surface electrons (which may mimic nuclear recoils because of inefficient charge collection) from bulk nuclear recoil events have further reduced significantly the number of nuclear recoil candidates above ~ 18 keV in the so-called FLIP detectors (CDMS)[40,41]. These remarkable results give confidence in this technique to reach the background levels sensitive for neutralinos searches.

3.4. Other discrimination techniques

They are based in the measurement of particle interaction parameters which are different for WIMPs than for the background. Some of these techniques are already working in prototypes or in running detectors. Others are still in project.

- Measuring the difference in ranges between nuclear and electron recoils in a detector medium (CASPAR)[42].

- Measuring the ratio of the Ultraviolet (UV) to Visible (VIS) light output in scintillators, which is different for nuclear and electron recoils (UVIS)[43].

- Identifying particle recoils in liquid Xenon by drifting the ionization to produce a second proportional scintillation pulse. The ratio between the primary (liquid Xenon direct scintillation) and secondary pulses is different for electron and nuclear recoils (ICARUS-like, ZEPLIN)[44].

- Using Superconducting Superheated Grains detectors (still in R+D phase) which are expected to provide a good discrimination for background rejection (estimated to be better than 97%), because a single grain is expected to flip per WIMP interaction in contrast to several grains for other radioactivity sources (PASS, ORPHEUS)[45].

- Using threshold detectors sensitive basically to neutron or nuclear recoils like the Superheated Droplets Detectors (SIMPLE)[46].

3.5. Results on Energy Thresholds

Some examples:

Visible (or electron equivalent) energy (corresponding to an effective nuclear recoil energy $\mathrm{T} = \mathrm{E_v}/\mathrm{Q}$

- 1.5 to 2 keV in Ge detectors (COSME[13], Caltech/PSI/UN[11], HDMS[25])
- 2 to 4 keV in NaI scintillators (DAMA[17], UKDMC[16], SACLAY[22])

Effective recoil energy (quenching factor Q $\sim$ 1)

- 0.3 to 0.5 keV in Al_2O_3 bolometers (CRESST[47], ROSEBUD[48])
- $\sim 2 - 8$ keV in large (340g) TeO_2 bolometers (MIBETA)[49]

  The charge and phonon noise produces a large increase of background at low energy, bringing the effective energy threshold up to 15–30 keV from the nominal 1 $\sim$ 3$\cdot$ keV in the running cryogenic detectors (CRESST[50], CDMS[41], EDELWEISS[51]).

3.6. Results on energy resolution

Some examples:

COSME [13]:	240 g Ge: $\Gamma = 0.5$ keV at 10 keV
DAMA [17]:	9.7 kg NaI: $\Gamma = 2$ keV at $10 - 50$ keV
CRESST [47]:	262 g Al_2O_3: $\Gamma = 0.25$ keV at 1.5 keV
	31 g Al_2O_3: $\Gamma = 0.1$ keV
ROSEBUD [48]:	25 g Al_2O_3: $\Gamma = 0.12$ keV at 1.5 keV
CDMS (BLIP) [6,41]:	100 g Si: $\Gamma = 900$ eV (thermal) and 450 eV (ionization)
CDMS (FLIP) [6,40]:	100 g Si: $\Gamma = 1$ keV thermal; $\Gamma = 3$ keV ionization
EDELWEISS [24,51]:	70 g Ge: $\Gamma \sim 1.2$ keV both thermal and ionization
MIBETA [49]:	340 g TeO_2: $\Gamma = 10$ keV at 2500 keV, $\Gamma = 2$ keV at $10 - 50$ keV

4. Prospects of running experiments, new detectors and future projects

We present a sample of a few detector projects which, following the above strategies and aiming to improve the achieved results, serve to illustrate the trends in

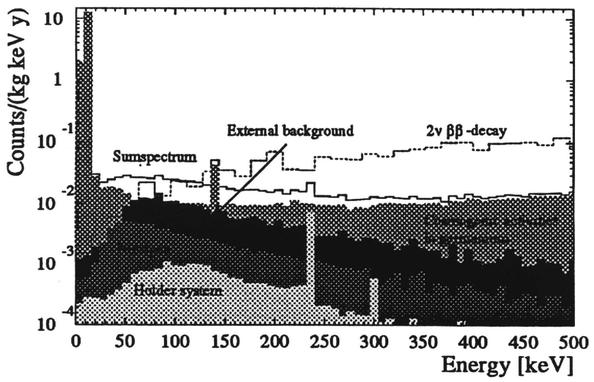

Figure 2: Montecarlo estimated background of the GENIUS detector project

future detection. The prospects of some of the experiments currently running is also reported.

4.1. Conventional Detectors

4.1.1. Ge Detectors

HDMS (Heidelberg Dark Matter Search)[25]. A small (200 g) Ge detector is placed in a well-type large (2 kg) Ge crystal (which acts as active veto of the small one) in a common crystal. The anticoincidence background suppression is estimated to be a factor $10-20$ (via Monte Carlo). Operation of the system in anticoincidence (not underground) gives a suppression factor of $5-6$. The goal of this experiment is to reach a background of B $\sim$ 0.01 c/keV kg day, down from the 0.1 c/keV kg day recent average background they obtained in the low energy region. These figures will allow to explore the region of the DAMA experiment.

GENIUS (Germanium Detectors in Liquid Nitrogen in an Underground Set-up)[26]. GENIUS is a project to operate a large set ($\sim$ 300) of naked germanium detectors (enriched in the isotope Ge-76), submerged directly in a tank of liquid nitrogen with the potential to look for physics beyond the standard model, in particular the double beta decay of ^{76}Ge. A small version of GENIUS plans to operate 40 natural abundance, naked germanium crystals (of 2.5 kg each), as a WIMPs detector. The set will be placed directly in a 12 m diameter, 9 m high tank of liquid Nitrogen to avoid material components of the detectors and so reduce further the background. The proof-of-principle of GENIUS (detectors operating directly in liquid nitrogen) has been already demonstrated. The very small radioimpurity contents of the GENIUS

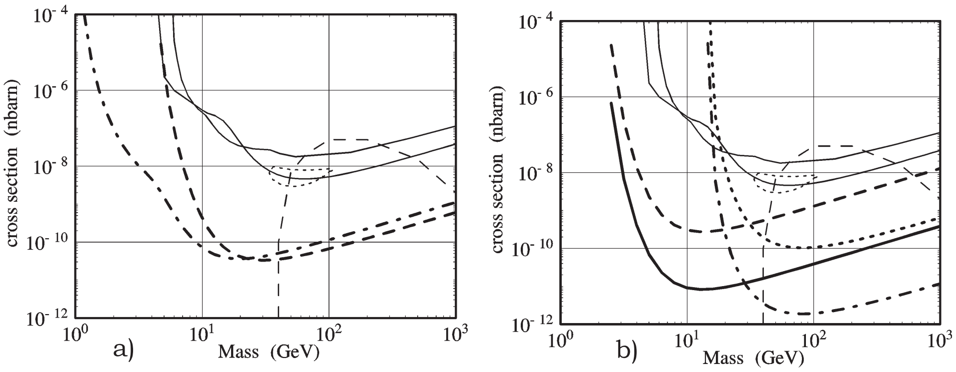

Figure 3: **(a)**Projections for CUORICINO (dot-dashed line) and GEDEON (thick dashed line) assuming the following paramters: MT = 42 kg y, E_{th} = 2 keV FWHM= 2 keV and b = 3×10^{-3} c/keV/kg/day for CUORICINO; and MT = 24 kg y, E_{th} = 2 keV, FWHM= 1 keV and b = 2×10^{-3} c/keV/kg/day for GEDEON. The regions enclosed by thin solid lines are the Ge-combined and DAMA excluded regions. The DAMA modulation experiment 2σ-allowed region (thin dots line) and MSSM region (thin dashed line) are also shown. **(b)** Projections for CDMS assuming two different sets of parameters: MT = 2 kg y, E_{th} = 2 keV, FWHM= 1 keV, b = 10^{-2} c/keV/kg/day (dashed line) (Stanford goal), and MT = 20 kg y, E_{th} = 2 keV, FWHM= 1 keV, b = 10^{-4} c/keV/kg/day (solid line) (Soudan goal); and for GENIUS, MT = 100 kg y, E_{th} = 10 keV, FWHM= 1 keV, b = 10^{-3} c/keV/kg/day (dots line), and, MT = 1000 kg y, E_{th} = 10 keV, FWHM= 1 keV, b = 10^{-5} c/keV/kg/day (dot-dashed line). The regions enclosed by thin solid lines are the Ge-combined and DAMA excluded regions. The DAMA modulation experiment 2σ-allowed region (thin dots line) and MSSM region (thin dashed line) are also shown.

components, hypothetically similar to that measured in the Counting Test Facility (CTF) of BOREXINO, have been used as inputs to MC estimate the background, which turns out to be B $\sim 3 \times 10^{-5}$ c/keV kg day, below 100 keV, the proposed goal of GENIUS. The MC estimated background of GENIUS is given in Fig. 2. The σ(m) expected plot explore most of the neutralino parameter space, as seen in the comparative exclusion plots of various current projected experiments depicted in Fig. 3b.

GEDEON (Germanium Diodes in One Cryostat, MOZA Collaboration, Canfranc)[27]**.** GEDEON is a detector project which uses the conventional, well-known, Ge-diode technology to look for cold dark matter. The GEDEON single cell is a cylindrical cryostat in electroformed copper (dimensions 20 cm diameter × 32 cm long) made with IGEX technology, hosting 28 (natural abundance) germanium crystals which share the same common copper cryostat (0.5 mm thick). A schematic view of the GEDEON single cell is shown in Fig. 4. The Ge crystals, of 860 g each, are arranged in four plates suspended from copper rods. The cell is embedded in a precision-machined hole in a Roman lead block providing a shield of 20 cm, surrounded by another lead shielding 20 cm thick. A cosmic veto and a neutron shield complete the shielding.

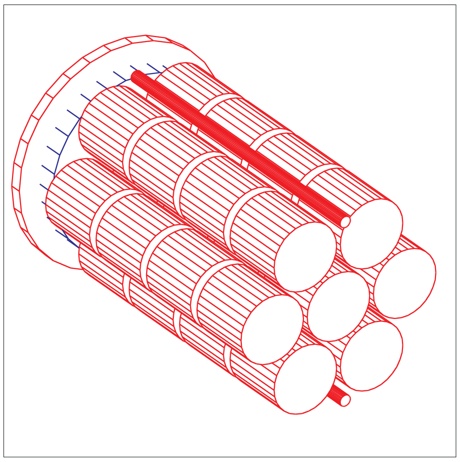

Figure 4: GEANT-generated picture of the GEDEON single cell (four planes of six 860 g Ge diodes). The single cryostat hosting the diodes is not shwown for clarity.

The preliminary MC estimated background in the $1 \sim 50$ keV region ranges from 2×10^{-2} to 2×10^{-3} c/keV kg day, according to the level of radioimpurities included as input. The radiopurity assays have been carried out in the Canfranc Laboratory for the lead and copper components of the shielding. The background goal of GEDEON, below 100 keV, is $\leq 10^{-3}$ c/keV kg day and this value has been used to calculate anticipated σ(m) exclusion plots. The expected threshold is $E_{thr} = 2$ keV and the energy resolution in the low energy region is $\Gamma \sim 1$ keV. The MC estimated background of the GEDEON unit cell (28 crystals) and predicted σ(m) plots are given Figs. 5a and 5b where it can be seen the region of the neutralino parameter space which GEDEON attempts to explore. The study design of this project is being performed, including also a second phase with four cryostats (112 detectors and a total mass of 92 kg of Ge).

4.1.2. Scintillators

Two large mass NaI scintillator experiments are running. DAMA in Gran Sasso, featuring ~ 100 kg, and ELEGANTS in Oto (Japan) with 730 kg. Both Collaborations are also operating other scintillator detectors like CaF_2. Results of DAMA and ELEGANTS can be found in other contributions to these Proceedings. New experiments or extensions of previous searches with scintillators are presented in the following.

ANAIS (Annual Modulation with NaIs, Zaragoza University, Canfranc)[54] . ANAIS is a large mass scintillators experiment planned to investigate seasonal modulation effects of WIMPs. It consists of 10 NaI hexagonal crystals (10.7 kg each) within an electroformed copper and Roman lead double box, which are coupled through light guides to ultralow background photomultipliers placed outside the internal shielding and cooled through Peltier devices. The shielding consists (from inside to outside) of 10 cm of Roman lead, 20 cm of low-activity lead, 2 m of cadmium and from 20 to 40 cm of polyethylene and water. A sealed box in PVC maintained at overpressure by the injection of 200 l/h of N_2 prevent the intrusion of Radon. An active veto is covering the set-up, which is being installed in the Canfranc Underground Laboratory at 2450 m.w.e. A schematic view of the ANAIS experimental setup can be seen in Fig. 6.

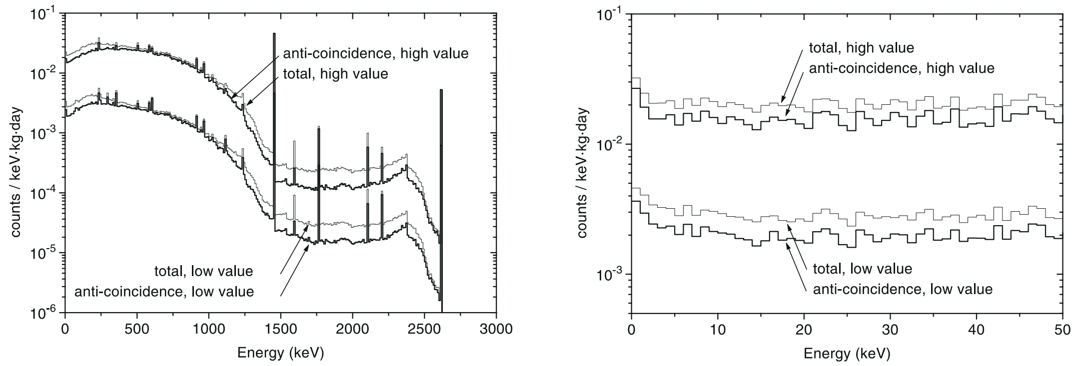

Figure 5: **(a)** Montecarlo estimated background of the GEDEON detector project (energy interval 0—3 MeV). **(b)** Montecarlo estimaged background of the GEDEON detector project (energy interval 0—50 keV).

The acquisition system records the events fired in each crystal, registering their energies and times (with an accuracy better than 1 second along the overall experiment). Anticoincidence pulses are recorded with digitizers for Pulse Shape Discrimination. Monitoring and stabilisation control of the experimental parameters (essential for modulation searches) will be particularly cared for. The expected performances are: energy threshold ~ 2 keV, and a background of about 2 c/keV kg day in the low energy region. This experiment is being prepared and partially installed for preliminary tests.

NaI UKDMC Program (Boulby)[16,52,53]**.** The UKDM Collaboration is carrying out a vast program of WIMP searches with NaI and other detectors in the Boulby mine. The experiments use radiopure NaI crystals of various masses (2 to 10 kg), with PMT and Silica light guides in various shielding conditions (water, lead, copper), and endowed with pulse shape discrimination readout for statistical background reduction.

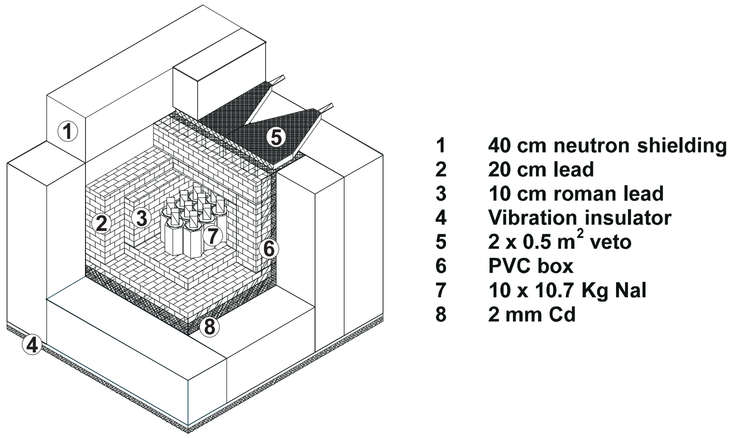

Figure 6: Schematic view of the ANAIS experimental set-up.

Recent results from a 5-kg NaI crystal with improved stability and energy resolution operating at $\sim T = 10°\mathrm{C} \pm 0.1°\mathrm{C}$ show (Fig. 7) a small population of pulses of average time constant shorter (230 ns) than that of the gamma events ($\sim$ 360 ns), and near to that corresponding to neutron-induced recoils, which has been proved not to be an instrumental artifact (nor due to alpha particles). No explanation to this unknown population has been found so far, but their impact in the differential spectrum has prevented till now to deduce safely σ(m) exclusion plots which should have improved—almost one order of magnitude—the exclusion previously obtained by this Collaboration. It is also worth to mention that it appears to be a significant summer-winter difference in that population. An interpretation in terms of WIMPs would require heavy WIMPs and some tuning of the halo velocity parameters.

Plans of UKDMC obviously include to clarify the origin of those events, and to investigate with various NaI and different conditions the possible faking of WIMP signals. For that purpose, they are using a NaI diagnosis array of a total of $\sim$ 20 kg (targets of different sizes, data acquired over different energy ranges, different shieldings).

The NAIAD system (NaI Advanced Detector) is a further step in this Program. NAIAD is a set of NaI detectors of a total mass of $50 - 100$ kg (under construction) which will use unencapsulated crystals to avoid surface problems and improve light collection, with all detectors using pulse shape analysis. The predicted sensitivities can be seen in Fig. 8.

Liquid Xenon ZEPLIN Program (UKDMC, Boulby)[44,53). The UKDM Collaboration, together with other groups, are developing and testing liquid Xenon detectors for WIMP searches to capitalize the better background discrimination provided by LqXe in comparison with that of the NaI pulse. Liquid Xenon produces scintillation and ionization, mechanisms which are used to discriminate nuclear recoils from

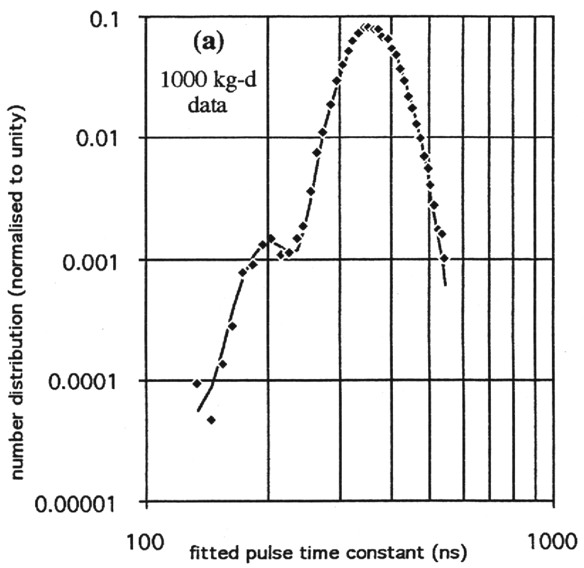

Figure 7: Average time constant distribution of data recorded with a NaI detector (UKDMC).

background events. The ZEPLIN I detector (UKDMC) features $\sim$ 4 kg of liquid Xenon in a vessel observed with three PMT and surrounded by a liquid scintillator veto and a lead shielding. ZEPLIN I will use PSD and the discrimination is achieved by allowing the scintillation to promptly recombine, adding to the scintillation light and giving differences in the scintillating pulse shape. This detector is ready to run at Boulby.

A further step, planned for 2001, is ZEPLIN II (UKDMC/UCLA/CERN/Torino/ ITEP) which plans to construct and operate a two-phase (liquid-gas) Xenon chamber of $10-20$ kg with ionization plus scintillation. The proof-of-principle of this detector

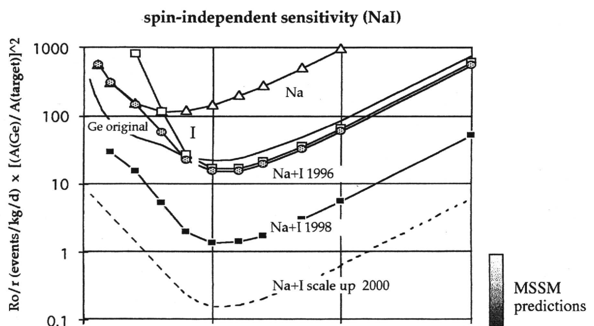

Figure 8: Predicted sensitivity of the NaI detector program (UKDMC). The variable plotted in the vertical axis is proportional to the cross-section.

has been demonstrated by UCLA/CERN. The nuclear recoil discrimination is due to the different ratio of secondary to primary scintillation pulses for nuclear recoils and gamma. An electric field is used to prevent the recombination, the charge being drifted to create a second scintillation pulse S_2 in addition to the primary pulse S_1 (the secondary scintillation is smaller for nuclear recoils). In the two-phase model, the charge is extracted from the liquid surface to the gas phase and accelerated to give a secondary pulse. The nuclear recoil discrimination in the UCLA/CERN test experiment can be seen in Fig. 9, and the projected sensitivity in Fig. 10.

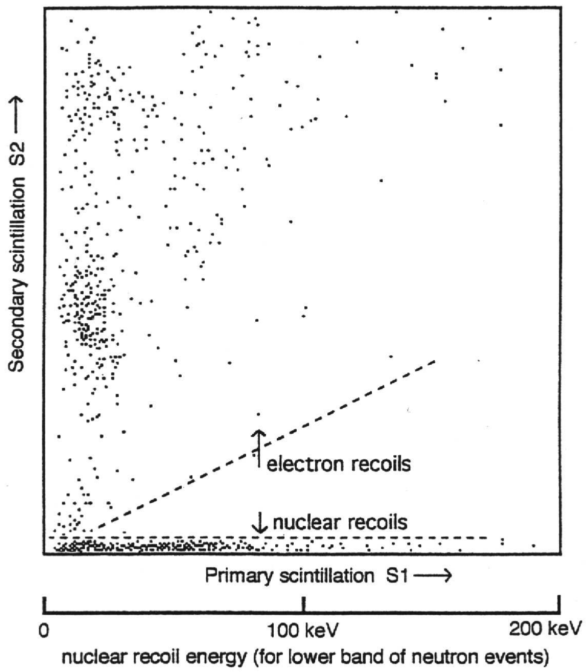

Figure 9: Nuclear and electron recoil discrimination obtained with the UCLA/CERN Xe detector prototype.

CASPAR (Cocktail with Alkali-Halide Scintillating particles, UKDMC, Boulby)[53,42). CASPAR consists of submicron grains of scintillating CaF_2 (Eu) suspended in an organic liquid scintillator matched to the same refractive index, where the discrimination between nuclear and electron recoils is achieved by measuring the differences in range of both types of recoil. The electron recoils (originated anywhere) will pass through both materials of the detector medium, giving a combined scintillation pulse containing two characteristic decay components ($\tau \sim 900$ ns and $\tau \sim 4$ ns). Nuclear recoils (of the same energy of the electron recoils) originate and remain in the grain (because of the enhanced cross-section and its much shorter recoil range), giving rise to one, slow scintillation pulse characteristic of CaF_2 (Eu). The discrimination is about 98%. The CASPAR performances for a detector of 10% volume filling factor

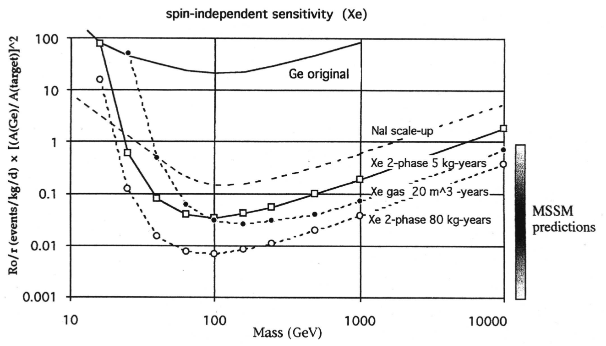

Figure 10: Predicted sensitivity of the future ZEPLIN detector.

with grains of 0.3 micron of diameter and a total mass of CaF_2 ~ 120 g, are expected to be $E_{thr} \sim 4$ keV and $B \sim 2$ c/keV kg day in this region.

The anticipated exclusion plots do not show essential improvements in SI plots with respect to that obtained with NaI. However, one order of magnitude improvement is expected in SD plots.

4.2. Cryogenic Particle Detectors[29)]

In the WIMP scattering on matter, only a small fraction of the energy delivered by the WIMP goes to ionization, the main part being released as heat. Consequently, thermal detectors should be suitable devices for dark matter and other rare event searches. Bolometers measure the increase of temperature produced in the absorbed by the recoiling target nucleus hit by a WIMP. The temperature pulse is detected with a sensor (like thermistors or superconducting phase transition thermometers) in thermal contact with the absorber. An appealing feature of these detectors is that their energy resolution should be a priori much better than that of conventional detectors, as the energy deposition mechanism is made in terms of phonons (10^{-4} – 10^{-6} eV). Cryogenic detectors fulfill many of the requirements needed for rare event Physics searches. They permit a wide choice of detector/target nuclei. Their efficiency is very good with quenching factors of about 100% and so they could provide detectors with low energy threshold needed for WIMPs searches. Finally, their capability to simultaneously measure the phonon and ionization (or scintillation) components of the energy deposition provides a unique tool of background subtraction and particle identification. In this last case, bolometers are currently referred as hybrid thermal detectors.

There exist five experiments on direct interactions of WIMPs based on thermal detection currently running (MIBETA, CDMS, EDELWEISS, CRESST, and ROSEBUD) and a big project, CUORE, in preparation.

Details and main results of these experiments are reported in the R. Bernabei's contribution to these Proceedings. We will sketch the latest developments and prospects

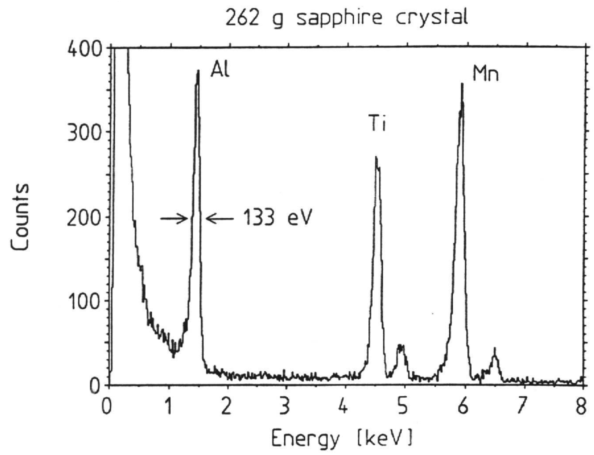

Figure 11: Energy spectrum of a 262 gr sapphire of CRESST obtained with an x-ray fluorescence source.

of these experiments, devoting particular attention to CUORE, as a large extension of the MIBETA array of crystals.

4.2.1. Bolometers

CRESST (MPI Munich/TUM Garching/Oxofrd, Gran Sasso)[47,50]. The CRESST (Cryogenic Rare Event Search using Superconducting Thermometers) detectors are four dielectric sapphire crystals (Al_2O_3) of 262 g each with a small superconducting film of tungsten evaporated onto the surface. This transition edge sensor is held at a temperature in the middle of its superconducting-to-normal conducting phase acting as a highly sensitive thermometer. The change of the film resistance produced by the WIMP (or particle) deposit of energy is measured with a SQUID.

The experiment has been running in Gran Sasso, with the bolometers placed inside a copper cold-box away from the dilution refrigerator by a cold finger 1.5 m long. The shielding surrounding the cold-box consists of 20 cm of lead and 14 cm of copper. The materials forming the cold-box and its enceinte have been recently substituted by low background components. The nominal energy threshold of the 262 g sapphire bolometer is 0.5 keV and the FWHM energy resolution at 1.5 keV is 133 eV (See Fig. 11). The background obtained in the Gran Sasso running is of a few counts/keV kg d above 30 keV, and 1 c/keV kg day is above 100 keV, whereas below 30 keV the spectrum is largely dominated by noise and other spurious sources. Improving the background below 30 keV as well as lowering the energy threshold actually obtained in the underground running are among the priorities for the immediate future of CRESST. Other prospects of CRESST include to try other absorbers (a germanium bolometer of 342 g is in preparation) and iridium-glod thermometers.

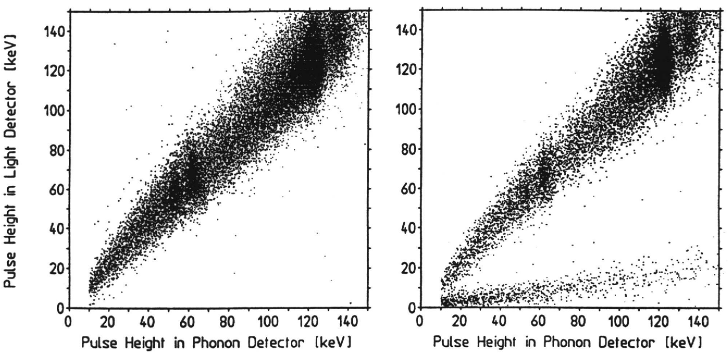

Figure 12: Phonon-scintillation discrimination obtained by the CRESST collaboration with a 6 g $CaWO_4$" bolometer and a small sapphire crystal.

New developments of this Collaboration[50)] are worth to be reported. Simultaneous measurement of scintillation and heat, with a 6 g $CaWO_4$ crystals as absorber, at 12 mK has been successfully performed, as an initial step of moving CRESST to hybrid detector. The preliminary results indicate a rejection of electron recoil events with an efficiency greater than 99.7% for nuclear recoil energies above 15 keV. See Fig. 12.

The short term (1999–2001) prospects for CRESST is the implementation of the scintillation-phonon discrimination of nuclear recoils in a $CaWO_4$ detector of 1 kg. The expectations for this device are based in an ambient background of B=1 c/keV kg day plus a rejection factor 99.7% above a recoil threshold of 15 keV

As long term prospects (2002 and beyond), CRESST intends to go to a total of 100 kg $CaWO_4$ detectors (the capacity of the experimental space of the cold box) with a background of B = 1 c/keV kg d further reduced by a rejection factor of f = 99.9% (above 15 keV). To fully explore the neutralino parameter space with 100 kg of $CaWO_4$, a background of 0.1 c/keV kg d plus a rejection factor of f = 99.99%, is needed together with a longer exposure (300 kg y), future final goal of CRESST.

ROSEBUD (IAS Orsay/Zaragoza University, Canfranc)[48)]. ROSEBUD (Rare Objects Search with Bolometers UndergrounD) is an experiment for exploring the low energy (300 eV–10 keV) nuclear recoils due to scattering of low mass WIMPs. It uses small sapphire bolometers (25 g to 200 g) of good energy resolutions (120 eV FWHM at 1.5 keV for a 25 g crystal) and very low thresholds ($\sim$ 300 eV) (Fig. 13). ROSEBUD has been installed in the Canfranc Underground Laboratory (Spain) at 2450 m water equivalent and has just started running. As a newcomer, it will be described in the following.

The first phase of the experiment consists of three small sapphire bolometers (two of 25 g and one of 50 g) operating inside a small dilution refrigerator (stick type, 6 cm diameter, 100 cm long). The Al_2O_3 bolometers are suspended (one above the other) inside an OFHC copper frame through nylon wires tensed to drive the

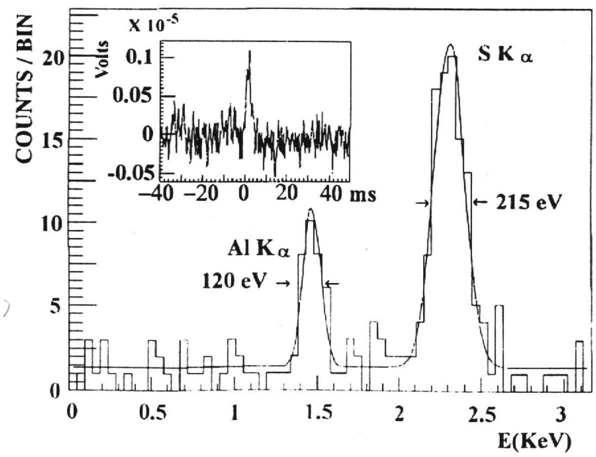

Figure 13: Energy spectrum of a 25 g sapphire bolometer of ROSEBUD obtained with an x-ray fluorescence source.

mechanical resonant frequency f_r to the highest possible value. The copper frames are mounted inside a copper structure coupled to the 20 mK mixing chamber of the dilution refrigerator. The thermal sensors are standard Neutron Transmutation Doped (NTD) germanium thermistors ($\sim$ 10 $-$ 15 mg) glued with epoxy to each crystal.

The inner shielding consists of especially melt Roman lead. This archaeological lead has very low contamination ($<$ 20 mBq/kg on ^{210}Pb and $<$ 0.2 mBq/kg on ^{238}U and $<$ 0.3 mBq/kg on ^{232}Th). A cylinder of such lead of dimensions similar to the bolometers (34.5 mm diameter and 30.8 mm height) is put on top of the 50 g sapphire to avoid the direct view of the dilution refrigerator components. On top of this lead cylinder there is a small LiF bolometer glued to the upper (25 g) sapphire crystal to measure the fast neutron flux during the experiment. A 1.5 mm thick lead piece at 20 mK is placed in the middle of the copper structure which fastens the bolometers and the lead cylinder. The archaeological lead inner shielding is completed by a 4 mm thickness can, placed at helium bath temperature around the bolometers block to shield the intrinsic radioactivity of the 0.5 cm thick stainless steel walls of the inner vacuum chamber. Surrounding the stainless steel cylinder (inside the helium bath) a 14.4 mm thick high purity copper piece shields the radioactivity of the metallic components of the refrigerator. The setting of the inner part of the dilution unit is depicted in Fig. 14a, whereas a general view of the setup is shown in Fig. 14b.

The refrigerator is placed in a liquid helium cryostat, entirely metallic, properly suspended to avoid microphonics. The external shielding (at room temperature) consists, from inside to outside, of 10 cm of Roman lead bricks and 15 cm of low-activity lead (70 yr. old, 30 Bq/kg of ^{210}Pb), forming a lead cube of $80 \times 80 \times 80$cm^3 (except for the hole where the DR enters the enceinte) enclosed in a plastic box

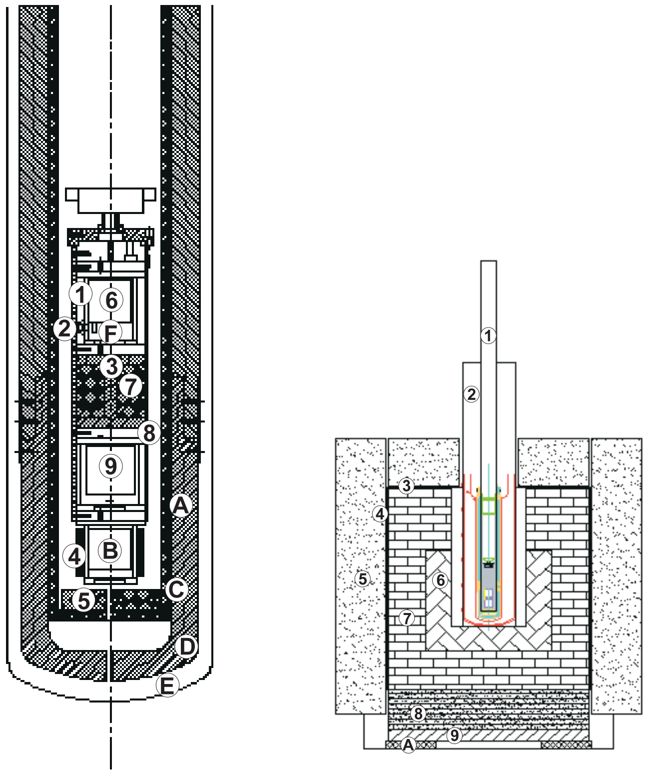

Figure 14: **(a)** Schematic view of the inner part of the ROSEBUD experimental set-up, showing the sapphire bolometers and inner shielding. **(b)** View of ROSEBUD set-up.

(silicone sealed) where nitrogen gas evaporated from a dewar is circulated to prevent the airborne radon penetration into the shielding. Notice that the radon level in the (air-ventilated) underground site ranges between 10 and 50 mBq/l, but it is reduced to $\sim 2.5 \times 10^{-2}$ mBq/l and stabilized inside the shielding of the experiment when flushed with nitrogen. The outmost part of the passive shielding is a neutron screen formed by a sheet of cadmium and a layer of 20 cm of paraffin and polyethylene. The experimental setup (Fig. 14b) is installed within an acoustics-insulated cabin, supported by an antivibration platform. The cabin is endowed with a Faraday cage. All the pumping, handling system and monitoring of the experiment is placed outside the experimental area. The first runs to test the bolometers on the underground site and the preliminary background measurements in different set-up conditions are being performed with encouraging results. A ^{57}Co source is intended for periodic energy calibration of the system. The stability is being monitored by means of IR pulses coming through optical fibers to the three bolometers (avoiding Joule heaters glued onto the crystals). A first running searching for WIMP dark matter will start shortly.

A thorough program of radiopurity measurements of the ROSEBUD components has been carried out with an ultralow background Ge detector in the same underground site, as well as in LSM Frejus. The results indicate that a background of $1 \sim 5$ c/keV kg day could be expected in the low energy region. Assuming a flat background of 1 count/keV kg day, a threshold energy of 300 eV and a FWHM resolution of 100 eV in the low energy region, a rough estimate of the expected sensitivity of the first phase of ROSEBUD is shown in Figs. 15 and 16, where the exclusion plots expected for spin-independent and spin-dependent coupling of neutralinos to ordinary matter are depicted. The quenching factor for the ROSEBUD sapphire bolometers is practically one ($Q = 0.98 \pm 0.05$ measured at 100 keV recoil energy[55]). The shaded area presents the theoretical prediction for the neutralino-nucleon cross section provided by an unconstrained Minimal Supersymmetric Standard Model (MSSM) where usual GUT relations among gaugino masses are relaxed[56].

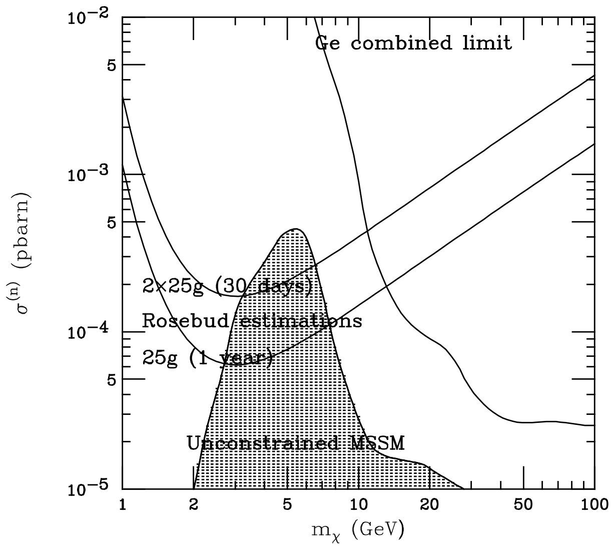

Figure 15: Expected σ(m) exlcusion plots of the ROSEBUD experiment for spin-independent coupling (assuming a flat background of 1 c/keV kg day, a threshold of 300 eV and an energy resolution of 100 eV)

As a first step, ROSEBUD is performing a series of short runnings in different conditions (of a duration of a few days each) to optimize the background, minimize microphonics and improve the performances of the bolometers, before going to larger running time. The next step will deal with two different bolometers (already prepared), one of 50 g of sapphire and one of 60 g of germanium, operating together to investigate the target dependence of the WIMP rate. A further step in this line of research is the use of two medium-size bolometers, 200 g Al_2O_3 (now ready) and 168 g germanium crystal (which is being prepared).

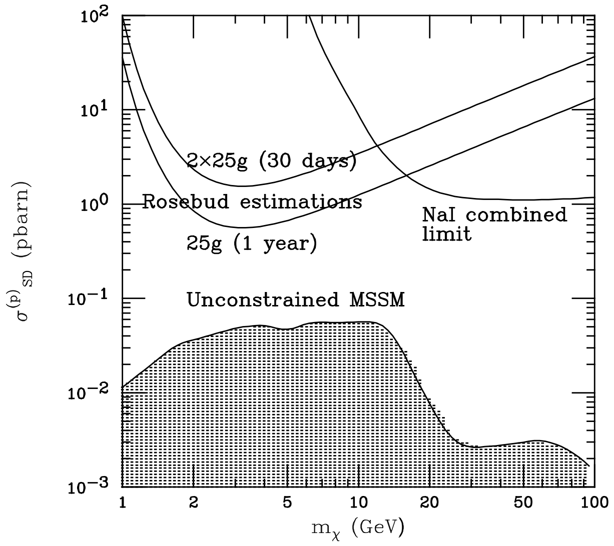

Figure 16: Same as in Fig. 15 for spin-dependent coupling

CDMS (Cryogenic Dark Matter Search, CfPA / UC Berkeley / LLNL/ UCSB / Stanford / LBNL / Baksan / Santa Clara / Case Western / Fermilab / San Francisco State)[6,23,40,41]. The Cryogenic Dark Matter Search Collaboration has been developing and testing for ten years hybrid bolometers which collect also electron-holes carriers, with the aim of discriminating nuclear recoils from electron recoils by the simultaneous measurement of the charge and phonons produced in absorbers of silicon and germanium by the WIMP scattering. Several detector prototypes have been running during short periods along the last years, to optimize the performances, the type of readout and to solve various new problems aroused in the course of their R+D program.

The ionization is measured by applying a small bias voltage ($\sim$few V/cm) through surface electrodes and using conventional charge amplifier technology. The electron-hole pairs are efficiently collected in the bulk of the detector, but the trapping sites near the detector surface produce a layer ($10-20\mu$m) of poor charge collection, where surface electrons from outside suffer ionization losses and fake nuclear recoils, spoiling so the effectiveness of the event discrimination technique. To solve this problem has been one of the main recent activities of the CDMS Collaboration. Their plans are first to minimize this soft electrons effect and then to optimize the phonon type of readout to establish finally which type of detector will be implemented at large scale for long runnings in an underground site.

Two types of phonon readout have been developed. In the BLIP (Berkeley Large Ionization and Phonon) detectors, a NTD Ge thermistor eutectically bounded to the absorber is used to read the thermal phonons in milliseconds. In the FLIP (Fast Large Ionization and Phonon) detectors, non-equilibrium, athermal phonons are detected

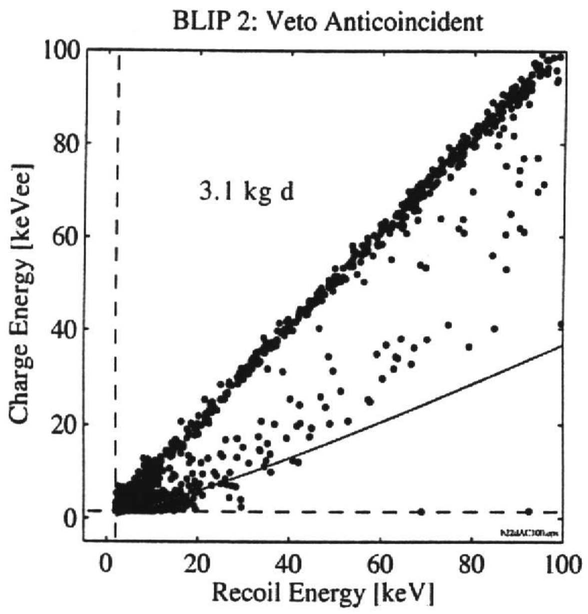

Figure 17: CDMS scatter plots of the ionization measurement normalized to electron equivalent energy versus the recoil energy measurement (with a 165 g Ge BLIP detector) in a 3.1 kg day background exposure. Note the soft electrons lying between this line and the diagonal photon line.

before thermalization. In this case, the sensors are tungsten superconducting transition edge thermometers (with electrothermal feedback) quasiparticle trap-assisted (QET technique). Current prototypes are BLIPs of 165 g Germanium and FLIPs of 100 g Silicon.

In the FLIP detectors, the microsecond time scale of phonon collection allows the localization of the events to define a detector fiducial volume away of the dead layer zone. To address the surface electrons problem, various successful strategies have been recently followed: i) the use of new electrodes for improving the charge collection. ii) the improvement in QET sensors design, which have resulted in an increase of the energy collection efficiency of one order of magnitude, and has lead to a new type of particle discrimination by phonon rise time: the low-charge collection events (surface electrons) have been proved to have faster phonon rise time ($4-5\mu$s) than the bulk events ($7-8\mu$s). A rise time cut (at 6.25μs) has been applied to discriminate between these two populations eliminating the soft-electrons.

The FWHM energy resolutions obtained are $\Gamma = 900$ eV and $\Gamma = 450$ eV respectively in the phonon and charge channels in BLIP detectors, and about 1 keV in FLIPs. The electron-nuclear recoils rejection in both detectors is larger than 99% above 20 keV recoil energy. Fig. 17 show the discrimination between nuclear and electron recoils in BLIP. The soft electrons can be seen between the two lines defining the gamma background (diagonal) and the nuclear recoil line. Fig. 18 shows the

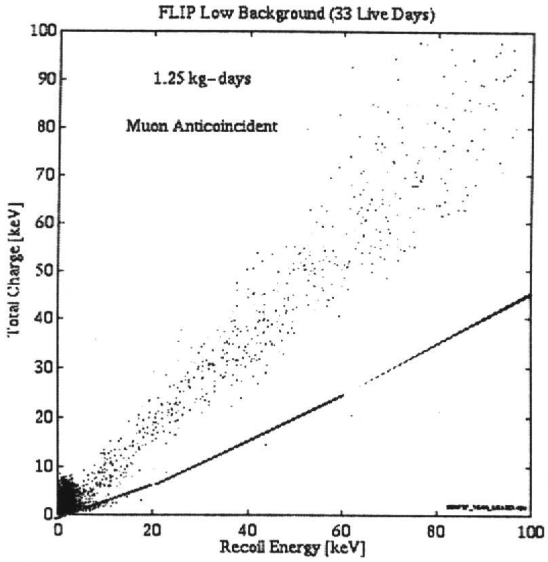

Figure 18: CDMS scatter plots for a background running (with a 100 g Si FLIP detector) where an athermal phonon risetime cut has been applied, eliminating the surface electrons.

FLIP performances[6,40]. A phonon rise time cut has been applied to elminate the surface electrons.

A recent running with four new 165 g Ge BLIP detectors featuring new charge electrodes has proved a better response to electrons than previous BLIPs, leading to much improved background rates[41]. The preliminary results show only one count due to nuclear recoil above $20-25$ keV recoil energy in 1.7 kg d exposure. See Fig. 19. These four BLIP detectors will take data for a few months during 1999, with a more compact geometry and with a germanium shield (besides the current shielding of the experiment, which consists of 1 cm of archaeological lead, a 25 cm thick layer of polyethylene and 15 cm of copper plus a muon veto).

Projects of the CDMS Collaboration include the transfer of the FLIP technology to germanium crystals, and so new FLIP Ge detectors of 250 g are being tested. The set of detectors which will be used for WIMP searches in Stanford will consist of two silicon FLIPs of 100 g and four germanium FLIPs of 250 g each, together with the current six germanium BLIPs of 165 g. Planned exposure at Stanford is of 100 kg day, with a background goal of B = 0.01 c/keV kg day.

In Stanford (17 m overburden), the sensitivity is limited by the ambient photon and neutron background. So, after achieving the goal of $\sim 10^{-2}$ counts/keV kg day, the experiment will be moved to Soudan along the year 2000. The project for SOUDAN is to assemble twenty FLIP detectors of Germanium (250 g each) with the background goal of B = few $\times\, 10^{-4}$ c/keV kg day. Fig. 3b shows the projected

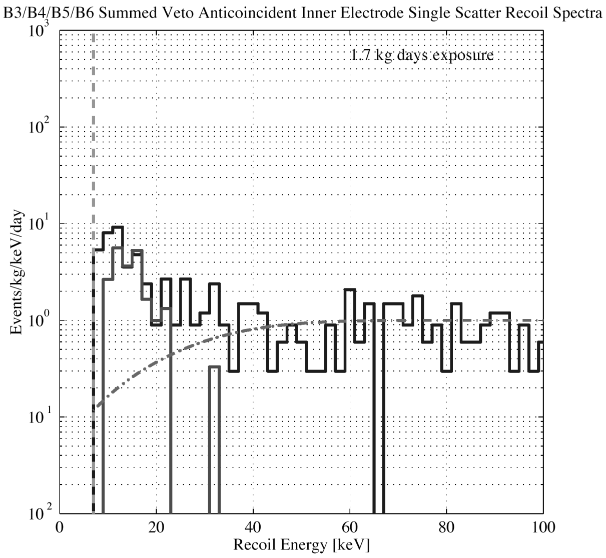

Figure 19: Energy spectrum of a CDMS recent run of four BLIP detectors with improved charge collection.

exclusion plots of CDMS (Stanford and Soudan), calculated with the best parameter values expected for this experiment, compared with those expected in other experiments. All the exclusions of Fig. 3a and 3b have been computed with the same set of halo parameters and method. The physics potential to explore the neutralino parameter space is also shown.

EDELWEISS (Orsay/Lyon/Saclay/LSM/IAP, Frejus)[24,51]. This collaboration has operated two 70 g HP Ge bolometer with heat-ionization discrimination with similar results to the BLIP detectors of CDMS. B = 0.6 c/keV kg day in $12-70$ keV in the recoil energy spectrum (1.17 kg day exposure). The rejection is 98% for surface events and $> 99.7\%$ for internal events.

The plans for 1999 are the preparation, first, of a small tower of three Ge bolometers of 70 g each, closely packed and then go to three Ge bolometers of 320 g with the objective of getting B $= 10^{-2}$ c/keV kg day. A second phase of EDELWEISS (2000–20001) will use a reverse DR (100 l) now under construction to host $50-100$ detectors where 20×300 g Ge detectors will be placed in the next two years, with the aim to improve rejection up to 99.99% and get B $\sim 10^{-4}$ c/keV kg day

CUORE (Cryogenic Underground Observatory for Rare Events) (Berkeley / Florence / LNGS / Leiden / Milan / Neuchatel / South Carolina / Zaragoza, Gran Sasso)[28,57,58]. CUORE is a project to construct a large mass (775 kg) modular detector consisting of 1020 single bolometers of (TeO_2) tellurite of dimensions $5 \times 5 \times 5$ cm^3 and 760 g each, endowed with glued NTD Ge thermistors,

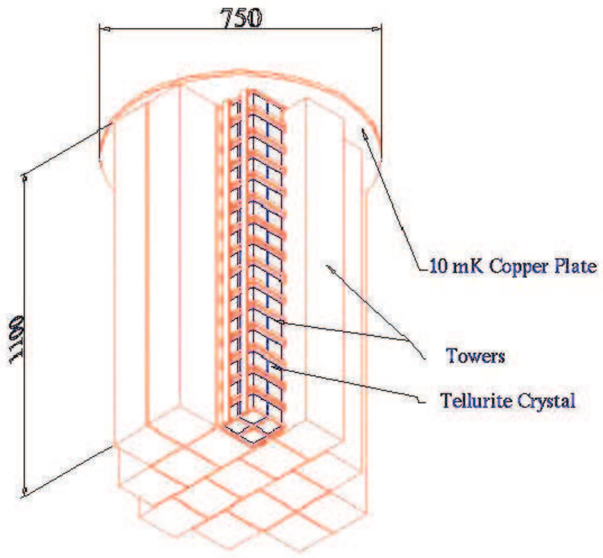

Figure 20: Schematic drawing of the tower-like structure of the CUORE crystals set-up. Only one tower of 15 planes is shown.

to be operated in a cryogenic facility in the Gran Sasso Laboratory. The features and expected performances of the CUORE bolometers array (large mass, high efficiency, good energy resolution and low energy threshold) will make it a powerful instrument to search for double beta decay of ^{130}Te, direct detection of WIMPs and other rare physics phenomena.

The detector will consist of seventeen towers in copper, each one containing fifteen planes, which are suspended from a copper plate (kept at about 7 $\sim$ 10 mK) within a dilution refrigerator. Each plane, which is the smallest independent detector unit, consists of four cubic TeO_2 crystals. The tower-like structure will enable each crystal to see almost completely all the surrounding ones and allow their operation in anticoincidence for background reduction. Fig. 20 shows a schematic drawing of CUORE. A single tower of 14 planes consisting of 56 crystals with a total mass of 42 kg, the so-called CUORICINO detector, will be a first step in the CUORE project.

CUORE benefits from the experience accumulated along many years by the Milano group in TeO_2 bolometers for rare event physics searches. Large bolometers of TeO_2 (334 g) with NTD Ge-sensors, (resolution of 1% at 60 keV and background of $\approx$ 12 counts/keV kg day at threshold, $E_{thr} \sim 10$ keV) have already constrained WIMPs and proved the sensitivity of these bolometers to nuclear recoils[15]. The nuclear recoil quenching factor Q of these bolometers has been measured to be $Q_{recoil} = 1.025 \pm 0.01(\mathrm{stat}) \pm 0.02(\mathrm{syst})$, independent of energy (from 10 to 200 keV)[59]. Various experiments have been performed with this type of bolometer at Gran Sasso, first with one bolometer, then with four crystals of 334 g each, and now a set of 20 crystals is

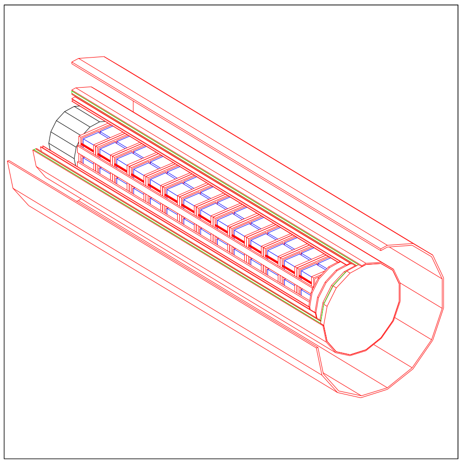

Figure 21: Montecarlo generated picture of CUORICINO tower.

running[49]. Preliminary results of the 20 crystal array (MIBETA experiment) allow to expect an energy threshold smaller than 5 keV and an energy resolution of $\sim 1-2$ keV in the few keV region[60]. CUORICINO and CUORE are designed as extensions of this array.

We will sketch in the following the main features, current status and expected performances of CUORICINO, a funded and approved experiment which will start the data taking in the LNGS by the beginning of year 2001.

The CUORICINO Experiment. CUORICINO consists of a set of 56 cubic tellurite crystals of 5 cm side and 760 g mass each, placed in a copper tower, which hosts four crystals per plane (See Fig. 21). The tower will be connected, via a copper cold finger, to the mixing chamber of the current MIBETA dilution refrigerator with minor modifications.

The CUORICINO tower will be topped with a Roman lead cylinder of 10 cm height and 15 cm diameter, which shields the intrinsic radioactivity of some components of the dilution unit. The external shield of the dilution refrigerator consists (from inside to outside) of a layer 2 cm thick of Roman lead (^{210}Pb content less than 4mBqkg^{-1}), then 20 cm of contemporary lead (^{210}Pb of 16 ± 4Bqkg^{-1}), and finally 10 cm of lead (^{210}Pb of 150 ± 20Bqkg^{-1}). The electrolytic copper of the thermal shields will provide an additional shield of 2 cm minimum thickness. The refrigerator is placed inside a Faraday cage.

The radiopurity of the main CUORICINO components (OFHC and electrolytic copper in the dilution refrigerator and tower and Roman and normal lead in the shields) have been measured with ultra low background Ge diodes operating in Gran Sasso and Canfranc. The upper limits of the radioimpurities range between 0.1 and 1 pg/g for uranium and potassium and between 1 and 10 pg/g for thorium, both for copper and lead, depending on the various material components. The tellurite crystals

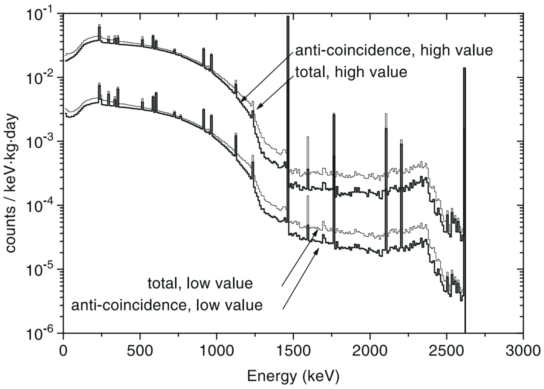

Figure 22: Montecarlo estimated background of CUORICINO (energy interval 0—3 MeV) (Preliminary).

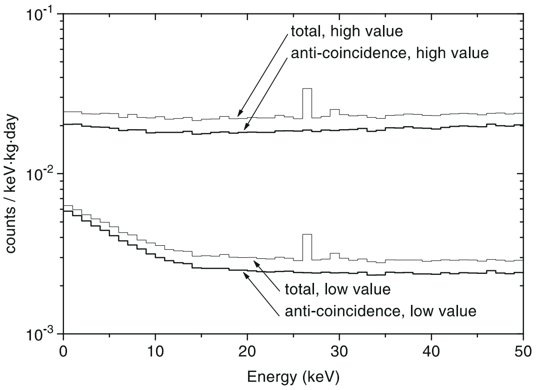

Figure 23: Montecarlo estimated background of CUORICINO (energy interval 0—50 keV) (Preliminary).

measured by Milan have thorium and uranium contents below 0.1 pg/g. These values have been used as inputs in a preliminary Monte Carlo simulation of the background using the GEANT program from CERN.

The corresponding expected background spectra in the low (dark matter) and high (neutrinoless double beta decay) energy regions are shown in Fig. 22 and 23, for the two cases of low and high measured upper limits of radioimpurity contents and with and without anticoincidence rejections. The diferential background count rates for the low ($1 - 50$ ke V) and high ($2400 - 2600$ keV) energy regions range between 3×10^{-3} and 2×10^{-2} c/keV kg day and between 2.5×10^{-3} and 2.2×10^{-2} c/keV kg year, respectively.

To optimize the bolometers performances with large absorbers like that of 760 g, specific studies on the NTD Ge thermistors properties and on the thermal couplings among the various elements which constitute the detector are required. A thermal model has been developed to predict the pulse structure of the bolometers. According to this model the thermistor volume must be increased by a factor of ~ 10 with respect to the MIBETA thermistor to obtain with a 760 g absorber a signal comparable or higher than that provided by the present 340 g crystals.

Two bolometers made with 760 g tellurite crystals, like the one shown in Fig. 24 following partially the prescriptions of the model have been recently tested in Gran Sasso using thermistors with the same doping, but with dimensions $3 \times 1 \times 3$ mm^3, 5 times larger than those used in the 20 crystal array. The spectrum of a ^{232}Th source is shown in Fig. 25. The preliminary results on the resolution in the region of neutrinoless double beta decay of ^{130}Te (2500 keV) is of about 10 keV, as shown in the Fig. 25. Recent results obtained after reducing vibrations lowers this value significantly. For instance resolutions of 1.3 keV at 352 keV, of 3.6 keV at 2615 keV and of 3.8 keV at 5400 keV, have been obtained[39)]

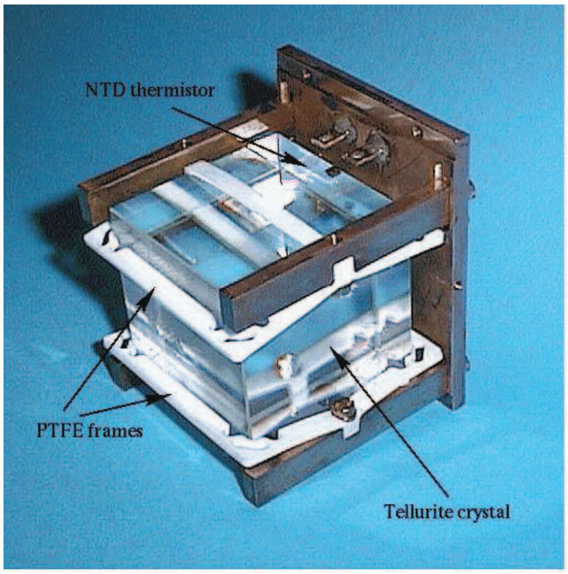

Figure 24: View of a CUORICINO crystal ($5 \times 5 \times 5cm^3$, 767.7 g) mounted for calibration measurements

The reproducibility of the current array of 20 bolometers of MIBETA can be seen in Fig. 26, where all the 20 contemporary calibration spectra with a single ^{232}Th source are reported. The sum of these spectra (see Fig. 27) shows that the array is indeed acting as a single detector. The same reproducibility is expected to be achieved with the 56 CUORICINO bolometers.

In the CUORE detectors (quenching factor about unit) a thermal and therefore effective threshold of 5 keV is expected. That would be equivalent to 1 keV in a germanium diode due to the relative quenching factor. Thresholds of 2 keV are very likely to be obtained. Notice that the MIBETA experiment has achieved in the very

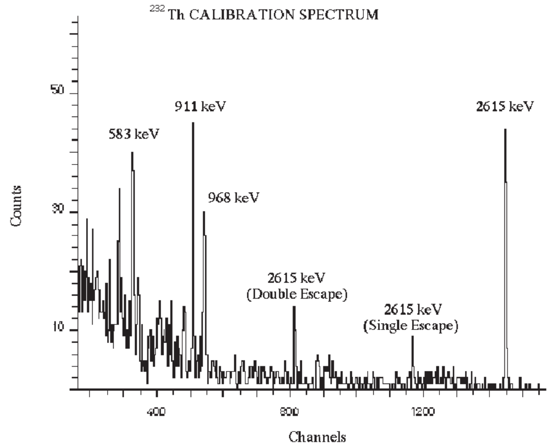

Figure 25: Calibration spectrum of the TeO_2, 767 g CUORICINO bolometer.

first runnings, energy thresholds ranging from 2 to 8 keV, depending on the detector.

In the anticoincidence mode, the low energy background expected in the CUORICINO array, together with such low energy threshold, will allow to significantly extend the regions of masses and cross sections explored for WIMP dark matter. In the very first runnings, MIBETA has reached background levels of a few counts per keV kg day in the low energy region[60]. On the other hand, the large mass of target make CUORICINO (and of course CUORE) a suitable tool in looking for annual modulation of WIMP signals. For reliable prospects of the sensitivities of CUORICINO in the seasonal modulation analysis, a better knowledge of long time stability and of systematic effects in the 20 detector array is essential. A preliminary estimate, nevertheless, allows to anticipate that with an exposure of CUORICINO of about 300 kg day, assuming a threshold of 2 keV and a backgroud of 0.1 c/keV kg day, the entire DAMA region could be explored. The Tellurium Oxide experiment has the added interest of using a different target from that used in the DAMA experiment and so would help in qualifying the type of WIMP-nucleus coupling of an hypothetical neutralino.

We show in Fig. 28 the expectations of CUORICINO/CUORE—in fact of a TeO_2 detector—for an exposure of 42 kg year and various low-energy (flat) backgrounds (assumed to be 1, 0.1 and 0.01 c/keV kg day). The threshold was set at 5 keV. Standard parameter values were used for the halo model, $\rho = 0.3$ GeV cm^{-3}, $v_{\rm rms} = 270{\rm Kms}^{-1}$ and $v_{\rm esc} = 650{\rm Kms}^{-1}$. According to the Monte Carlo estimation, the background figures are very conservative, even the last one. The accumulating statistics of the 20 detector array will help for a better estimation and a correct understanding of the background. In the comparative exclusion plots in Fig. 3a, the results obtained from running experiments (Ge, NaI), and the projections for GEDEON and CUORICINO are plotted. The scale is the same as in the plot of Fig. 3b, corresponding to the

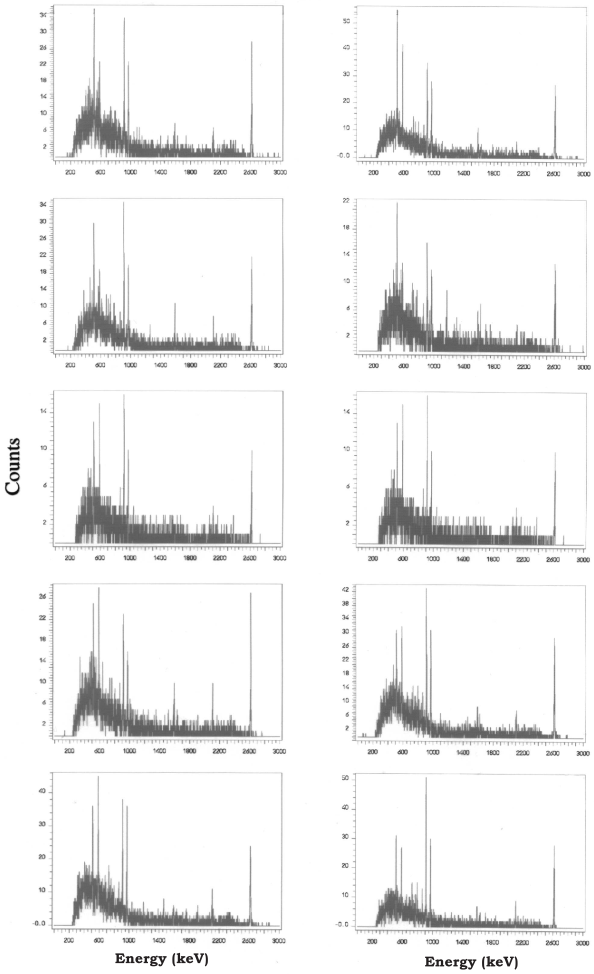

Figure 26: Calibration spectra of a set of TeO_2 crystals of the MIBETA array.

projection of CDMS and GENIUS. In the central part of Fig. 3a and b, a small banana-shaped region indicates the values of σ and m singled out by the reported DAMA effect. The background, threshold and energy resolution quoted for CUORE are the best figures expected for the experiment. As it can be seen, CUORICINO (and CUORE) will allow to explore a significant region of the neutralino parameter space[19)].

There exists other interesting capabilities of CUORICINO for doing rare physics research. It has been recently proposed to search for solar axions ($2-10$ keV energy range, peaked at 4 keV) by looking for their coherent Primakoff conversion into photons in crystal detectors[61,62)]. Detection rates in a germanium diode, for instance, would be enhanced if axions from the Sun coherently convert into photons when their incident angle with a given crystalline germanium plane fulfils the Bragg condition. This modulation of the rates would be correlated to the relative position of the lat-

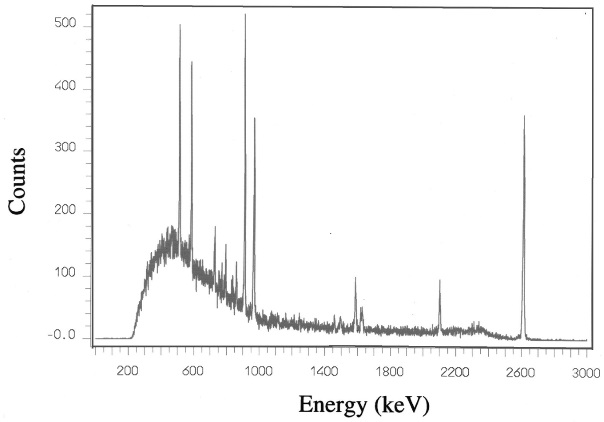

Figure 27: Summed spectrum of the twenty individual and contemporary 20 spectra of the MIBETA array.

tice planes of the detector with respect to the Sun, and would lead to a well defined rate variation pattern. An experiment has been already carried out by the SOLAX Collaboration (USC/PNNL/Zaragoza/Tandar)[63] with a germanium detector in the Sierra Grande mine (Argentina), getting an upper limit of $2.7 \times 10^{-9}\mathrm{GeV}^{-1}$ on the axion-photon coupling $g_{a\gamma\gamma}$. Another experiment, COSME (MOZA Collaboration), currently running at the Canfranc Tunnel, has reached a similar bound. The Milan group is also performing a solar axion search in the Gran Sasso Laboratory with the presently installed array of twenty TeO_2 crystal (MIBETA).

The use of TeO_2 crystals in CUORICINO/CUORE for solar axion searches could have some advantages with respect to germanium detectors, mainly because of the larger mass, and the fact that the cross-section for Primakov conversion depends on the square of the atomic number. However, instrumental performances and specific features of the TeO_2 crystal detectors limit the relative gain with respect to germaniums.

There are various astrophysical bounds on $g_{a\gamma\gamma}$ which set the sensitivity to be required in searches with crystal detectors. A recent bound[65] coming from helioseismological data (sound-speed profiles) sets $g_{a\gamma\gamma} < 10^{-9}\mathrm{GeV}^{-1}$ which is the minimal goal for planning a solar axion search. Even more restrictive is the globular cluster bound[64] $g_{a\gamma\gamma} \leq 6 \times 10^{-11}\mathrm{GeV}^{-1}$.

The sensitivity of an axion experimental search can be expressed as the upper bound of $g_{a\gamma\gamma}$ which such experiment would provide from the non-appearance of the axion signal for a given crystal, background, exposure, threshold and resolution. A conservative calculation of the axion-photon coupling bound $g_{a\gamma\gamma}$ achievable by the TeO_2 arrays of detectors (like MIBETA, CUORICINO, CUORE) due to this mechanism of axion-photon conversion, as well as by other experiments mentioned in this review (ANAIS, DAMA, GENIUS) has been recently done[66] with the result:

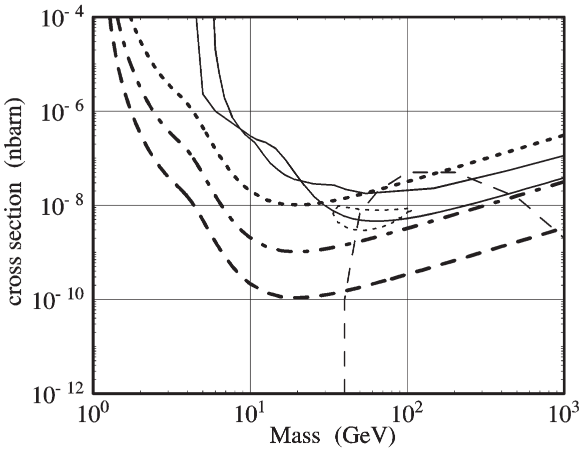

Figure 28: Cross-section versus mass predictions for CUORICINO assuming MT = 42 kg y, $E_{th} = 2$ keV, $\Gamma = 2$ keV and different backgrounds: B = 1 (dots), 0.1 (dot-dash) and 0.01 (dash) c/keV kg day. The region enclosed by thin solid lines are the Ge-combined and DAMA excluded regions. The DAMA 2σ-allowed region (thin-dots line) and MSSM region (thin-dashed line) are also shown.

$$g_{a\gamma\gamma} < g_{a\gamma\gamma}^{lim} \sim k \left(\frac{B}{c/\mathrm{keV\ kg\ day}} \frac{\mathrm{kg}}{\mathrm{M}} \frac{\mathrm{years}}{\mathrm{T}} \right)^{1/8} \times 10^{-9}\ \mathrm{GeV}^{-1} \tag{1}$$

Where k depends on the crystal structure and material, as well as on the experimental threshold and resolution. For instance, for CUORICINO k has been calculated to be 3.0 for an energy resolution of 2 keV, and 2.9 for an energy resolution of 1 keV from where a bound on the axion-photon coupling can be given according to the background.

Table 1 gives the prospects of axion searches for various future crystal detectors. A possible future Pb detector has been also included to give an indication of the ultimate limit with heavy elements to take advantage of the Z^2 factor in the cross-section. As it can be seen, crystals have no realistic chances to challenge the globular cluster limit, but the sensitivity required for crystal-detectors in order to explore a range of $g_{a\gamma\gamma}$, compatible with the solar limit is within reach.

Fig. 29 shows the current bounds in the plane $m_a - g_{a\gamma\gamma}$. The horizontal thick line represents the constraint $g_{a\gamma\gamma} \leq 3 \times 10^{-10}\mathrm{GeV}^{-1}$ corresponding to GENIUS. The mass intervals $m_a \leq 10^{-6}$ eV, 10^{-2}eV $\leq m_a \leq 3$ eV, $m_a \geq 20$ eV are excluded respectively by cosmological overclosure, SN1987A and oxygen excitation in water Cherenkov detectors, the edges of all the excluded regions being subject to many astrophysical and theoretical uncertainties. The horizontal lines represent the limits from SOLAX, helioseismology, and globular clusters. The theoretical predictions for $g_{a\gamma\gamma}$ in the case of the DFSZ and the KSFZ axion models are also given.

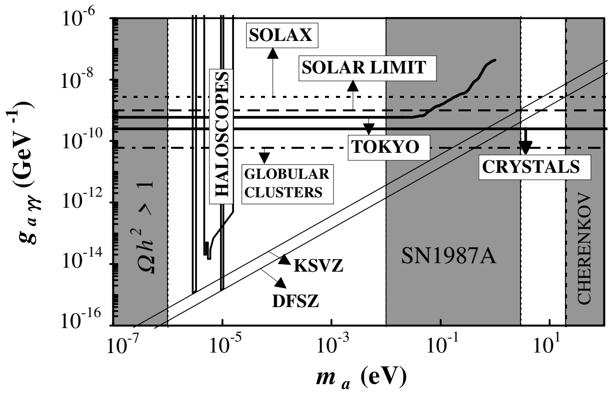

Figure 29: Bounds in the plane axion-foton coupling $g_{\gamma\gamma}$ versus axion mass m_a (See text).

Table 1: Axion search sensitivities for running (DAMA), being installed (CUORICINO, ANAIS), and planned (CUORE, GENIUS) experiments are compared to the result of SOLAX.

		K	M	B	E_{th}	FWHM	$g_{a\gamma\gamma}^{lim}$ (2 yrs)
			(kg)	(cpd/kg/keV)	(keV)	(keV)	(GeV^{-1})
SOLAX	Ge	2.5	1	3	4	1	2.7×10^{-9}
GENIUS	Ge	2.5	1000	1×10^{-4}	4	1	3×10^{-10}
CUORICINO	TeO_2	3	42	0.1	5	2	1.3×10^{-9}
CUORE	TeO_2	2.8	765	1×10^{-2}	3	2	6.3×10^{-10}
DAMA	NaI	2.7	87	1	2	2	1.4×10^{-9}
ANAIS	NaI	2.8	107	2	4	2	1.6×10^{-9}
	Pb	2.1	1000	1×10^{-4}	4	1	2.5×10^{-10}

5. Acknowledgements

I am indebted to Milla Baldo-Ceolin for her kind invitation to give this talk and for creating such a stimulating and warm atmosphere in this remarkable series of Venice Workshops. I wish to thank Pierluigi Belli, Rita Bernabei, Chiara Brofferio, Maurice Chapellier, Gabriel Chardin, Noel Coron, David Caldwell, Ettore Fiorini, Hirojasu Ejiri, Andrea Giuliani, Sunil Golwala, Maura Pavan, Franz Proebst, Marisa Sarsa, Wolfgang Seidel and Neil Spooner, for information about the results of their experiments and future projects, as well as for the figures provided. I am indebted to my collaborators Eduardo García, Igor G. Irastorza and Stefano Scopel for their collaboration in the making of the exclusion plots and to the last two, in particular, for discussions on the annual modulation sensitivity and solar axion prospects of

CUORICINO. I am also indebted to Susana Cebrián and David González for their unvaluable help in the Montecarlo estimation of GEDEON and CUORICINO expected backgrounds. Thanks are due to Alfonso Ortiz for his drawing of some of the figures. Valuable discussions with Julio Morales on several experimental aspects of the reported works are also acknowledged. The patient and careful typesetting of the text by Mercedes Fatás is warmly appreciated. This work has been supported by the Joint Committee for the Scientific and Technological Cooperation between Spain and the United States of America, the EU Network on Cryogenic Detectors ERB-FMRX-CT98-0167, as well as by the Spanish Agency on Science and Technology, CICYT, under grant AEN98-0627.

6. References

1) B. Lee and S. Weinberg, *Phys. Rev. Lett.* **39** (1977) 165; J. Silk and M. Srednicki, *Phys. Rev. Lett.* **39** (1984) 624; G. Jungman, M. Kamionkowski and K. Griest, *Phys. Rep.* **267** (1996) 195; J.R. Primack, D. Seckel and B. Sadoulet, *Ann. Rev. Nucl. Part. Sci.* **38** (1988) 751.
2) R. Peccei and H. Quinn, *Phys. Rev. Lett.* **38** (1977) 1440; M.S. Turner, *Phys. Reports* **197** (1990) 167; P. Sikivie, *Phys. Rev. Lett* **51** (1983) 1415; G. Raffelt, *Phys. Rep.* **198** (1990) 1.
3) M.W. Goodman and E. Witten, *Phys. Rev.* **D31** (1985) 3059; J.R. Primack, D. Seckel and B. Sadoulet, *Ann. Rev. Nucl. Part. Sci.* **38** (1988) 751.
4) P.F. Smith and J.D. Lewin, *Phys. Rep.* **187** (1990) 203.
5) G. Jungman, M. Kamionkowski and K. Griest, *Phys. Rep.* **267** (1996) 195.
6) B. Sadoulet, "Direct Searches for Dark Matter", in Proc. XVIII Intl. Conf. on Neutrino Physics and Astrophysics, Neutrino 98, (Takayama, Japan, 1998), ed. Y. Suzuki and Y. Totsuka., *Nucl. Phys. B (Proc.Suppl.)* (1999).
7) D.O. Caldwell, *Nucl. Phys. B (Proc. Suppl.)* **70** (1999) 43.
8) A. Morales, *Nucl. Phys. B (Proc. Suppl.)* **70** (1999) 54 and "Particle Dark Matter and its Detection", Summary Talk at NuPECC Workshop on Present and Future of Neutrino Physics in Europe, Frascati 1996, Preprint: astro-ph/9810341.
9) S.P. Ahlen et al., *Phys. Lett.* **B195** (1987) 603.
10) D.O. Caldwell et al., *Phys. Rev. Lett.* **61** (1988) 510.
11) D. Reusser et al., *Phys. Lett.* **B235** (1991) 143.
12) M. Beck et al., *Phys. Lett.* **B336** (1994) 141; L. Baudis et al. *Phys. Rev.* **D59** (1999) 022001.
13) E. García et al., *Phys. Rev.* **D51** (1995) 1458; J. Morales et al., *Nucl. Instr. and Methods* **A321** (1992) 410.
14) A. de Bellefon et al., *Nucl. Instr. and Methods* **A370** (1996) 230.
15) A. Alessandrello et al., *Phys. Lett.* **B384** (1996) 316 and *Nucl. Instr. and*

Methods **A370** (1996) 241.
16) P.F. Smith et al., *Phys. Lett.* **B379** (1996) 299; J.J. Quenby et al., *Astrop. Phys.* **5** (1996) 249.
17) R. Bernabei et al., *Phys. Lett.* **B389** (1996) 757.
18) R. Bernabei et al., *Phys. Lett.* **B424** (1998) 195, Rome II preprint: ROM2F/98/34 and INFN/AE-8/23.
19) A. Bottino, et al., *Phys. Lett.* **B423** (1998) 109; *Phys. Rev.* **D59** (1999) 095003, *ibid* 095004; and *Astrop. Phsy.* **10** (1999)203; S. Scopel and N. Fornengo, private communication. See also A. Bottino, these Proceedings.
20) A. Bottino et al., *Astrop. Phys.* **2** (1994) 77; *ibid* **3** (1995) 65; and *Phys. Lett.* **B402** (1997) 113.
21) H.E. Haber and G.L. Kane, *Phys. Rep.* **117** (1985) 75.
22) G. Gerbier et al., "Pulse Shape Discrimination and Dark Matter Search with NaI Scintillators", Preprint: DAPNIA/SPP98-11.
23) T. Shutt et al., *Phys. Rev. Lett.* **29** (1992) 3425; P.D. Barnes et al., *J. Low Temp. Phys.* **93** (1993) 79; D.S. Akerib et al., *Nucl. Phys. B (Proc. Suppl.)* **70** (1999) 64; S.W. Nam et al., in Proc. Workshop on Low Temperature Detectors, LTD-7 (Munich 1997), ed. S. Cooper (Pub. Max Planck Institute, Munich 1997) p. 217; J.J. Gaitskell et al., *ibid* p. 221; A.K. Davies et al., *ibid* p. 227; R.M. Clarck et al., *ibid* p. 229; A. Sonnenschein, "Results of the CDMS obtained with thermistor-instrumented Ge calorimeters", in Proc. Workshop on the Identification of Dark Matter (England, 1997), ed. N. Spooner (Pub. World Scientific, Singapore 1999); B. Sadoulet in Ref. [6] and references therein.
24) D.L'Hote et al., *Nucl. Instrum. and Methods* **A370** (1996) 193; D.L. Hote et al., in Proc. Workshop on Low Temperature Detectors, LTD-7 (Munich 1997), ed. S. Cooper (Pub. Max Planck Institute, Munich 1997) p. 237; L. Berge et al., *Nucl. Phys. B (Proc. Suppl.)* **70** (1999) 69.
25) L. Baudis et al., *Nucl. Phys. B (Proc. Suppl.)* **70** (1999) 106.
26) J. Hellmig and H.V. Klapdor-Kleingrothaus, *Zeit. fur Phys.* **A359** (1997)351; H.V. Klapdor-Kleingrothaus, GENIUS, Prepring: hep-ex/9802007.
27) A. Morales et al., GEDEON, a project for WIMP searches with a set of natural abundance Ge diodes in a single cryostat. Preliminary Study for Submission to CICYT (Spain), January 1999.
28) CUORE, A Cryogenic Observatory for Rare Event Searchers Letter of Intent submitted to INFN, September 1997; CUORICINO Proposal to the Committee of the LNGS and to the Funding Authorities, 1998.
29) N. Booth, B. Cabrera and E. Fiorini, *Ann. Rev. of Nucl. Sci.* **46** (1996) 471; E. Fiorini, *Nucl. Phys. B (Proc. Suppl.)* **48** (1996) 41.
30) J. Ellis and R.A. Flores, *Phys. Lett.* **B263** (1991) 259.
31) J.D. Lewin, P.F. Smith, *Astrop. Phys.* **6** (1996) 87.
32) J. Engel, *Phys. Lett.* **B264** (1991) 114; J. Engel, S. Pittel and P. Vogel, *J.*

Int. Mod. Phys. **E1** (1992) 1; J. Engel et al., *Phys. Rev.* **C52** (1995) 2216; J. Engel and P. Vogel, *Phys. Rev.* **D40** (1989) 3132; M.T. Ressel and D.J. Dean, Preprint hep-ph/9702290 (Feb. 1997); M.T. Ressel et al., *Phys. Rev.* **D48** (1993) 5519.

33) A.K. Drukier, K. Freese and D.N. Spergel, *Phys. Rev.* **33** (1986) 3495; K. Freese, J. Frieman and A. Gould, *Phys. Rev.* **D37** (1987) 3388.
34) D.N. Spergel, *Phys. Rev.* **D37** (1988) 353.
35) M.L. Sarsa et al., *Nucl. Phys. B (Proc. Suppl.)* **48** (1996) 73; *Phys. Lett.* **B386** (1996) 458; *Phys. Rev.* **D56** (1997) 1856.
36) P. Belli et al., *Phys. Lett.* **B387** (1996) 222; Erratum, *Phys. Lett.* **B389** (1996) 783.
37) K. Fushimi et al., *Phys. Rev.* **C47** (1993) R425; H. Ejiri, Proc. XVII Intl. Conf. on Neutrino Physics and Astrophysics, Neutrino 96, (Helsinki, 1996), ed. K. Enqvist, K. Huitu, J. Maalampi (Pub. World Scientific, Singapore 1997) p. 342.
38) A.K. Drukier et al., *Nucl. Phys. B (Proc. Suppl.)* **28A** (1992) 293.
39) E. Fiorini, private communication, May 1999.
40) R.M. Clarke, "Results of the CDMS obtained using a new athermal phonon mediated detector", in Proc. Workshop on the Identification of Dark Matter, IDM98 (Buxton, England, 1998), ed. N. Spooner (Pub. World Scientific, Singapore 1999).
41) D.O. Caldwell and S.R. Golwala, private communication.
42) D.R. Tovey, *Nucl. Phys. B (Proc. Suppl.)* **70** (1999) 111 and N. Spooner, private communication.
43) N.J. Spooner and P.F. Smith, *Phys. Lett.* **B314** (1993) 430.
44) P. Benetti et al., *Nucl. Instrum. and Methods* **A237** (1993) 203; J. Park et al., in Proc. Workshop on Sources of Dark Matter in the Universe, ed. D. Cline (Pub. World Scientific, Singapore, 1994) p. 288.
45) B.G. Turrell, "Introduction to SSG Detectors" in Proc. VII Int. Workshop on Low Temperature Detectors (Munich, 1997), ed. S. Cooper (Pub. Max Planck Institute, Munich 1997) p. 188.
46) J.I. Collar, *Phys. Rev.* **D54** (1996) R1247.
47) M. Sisti et al., in Proc. VII Int. Workshop on Low Temperature Detectors (Munich, 1997), ed. S. Cooper (Pub. Max Planck Institute, Munich 1997) p. 232; L. Zerle et al., *Nucl. Phys. B (Proc. Suppl.)* **70** (1999) 74.
48) C. Bobin et al., *Nucl. Phys. B (Proc. Suppl.)* **70** (1999) 90.
49) A. Alessandrello et al., *Phys. Lett.* **B433** (1998) 156.
50) M. Bravin et al., "The CRESST Dark Matter Search Proposal to the Gran Sasso Laboratory ", 1998; M.L. Sarsa, F. Proebst and W. Seidel, private communication, February 1999.
51) G. Chardin, private communication, February 1999.

52) P.F. Smith et al., *Phys. Rep.* **307** (1998) 275.
53) N. Spooner, private communication, February 1999.
54) E. García et al., in Proc. XXV Intl. Meeting on Fundamental Physics (Formigal, Spain, 1997), ed. M. Aguilar, E. Fernández, A. Morales, F. Ynduráin (Pub. World Scientific, Singapore, 1998) p. 225.
55) J.W. Zhou et al., *Nucl. Instrum. and Methods* **A349** (1994) 225.
56) A. Gabutti et al., *Astrop. Phys.* **6** (1996) 1.
57) O. Cremonesi, in Proc. XVIII Intl. Conf. on Neutrino Physics and Astrophysics, Neutrino 98, (Takayama, Japan, 1998), ed. Y. Suzuki and Y. Totsuka., *Nucl. Phys. B (Proc.Suppl.)* (1999).
58) C. Brofferio and A. Giuliani, private communication.
59) A. Alessandrello, *Nucl. Phys. B. (Proc. Suppl.)* **70** (1999) 96.
60) E. Fiorini and M. Pavan, private communication, February 1999.
61) E.A. Pascos and K. Zioutas, *Phys. Lett.* **323** (1994) 367.
62) R.J. Creswick et al., *Phys. Lett.* **B427** (1998) 235.
63) F.T. Avignone et al., *Phys. Rev. Lett.* **81** (1998) 5068.
64) H. Schlattl, A. Weiss and G. Raffelt, "Helioseismological constraint on solar axion emission", Prepring: hep-ph/9807476, July 1998.
65) G. Raffelt, "Axion hunting at the turn of the Millenium" in Proc. XVIII Intl. Conf. on Neutrino Physics and Astrophysics, Neutrino 98, (Takayama, Japan, 1998), ed. Y. Suzuki and Y. Totsuka., *Nucl. Phys. B (Proc.Suppl.)* (1999).
66) S. Cebrián et al., *Astrop. Phys.* **10** (1998) 397.